Extrapolating the evolution of galaxy sizes to the epoch of reionization

Monthly Notices of the ROYAL ASTRONOMICAL SOCIETY LETTERS

Mon. Not. R. Astron. Soc. **413,** L38–L42 (2011) doi:10.1111/j.1745-3933.2011.01027.x

Extrapolating the evolution of galaxy sizes to the epoch of reionization

J. Stuart B. Wyithe[1⋆] and Abraham Loeb[2⋆]

[1]*School of Physics, University of Melbourne, Parkville, Victoria, Australia*
[2]*Astronomy Department, Harvard University, 60 Garden Street, Cambridge, MA 02138, USA*

Accepted 2011 February 2. Received 2011 February 1; in original form 2010 December 19

ABSTRACT

We use data on the high-redshift evolution of the size distribution and luminosity function of galaxies to constrain the relationship between their star formation efficiency and starburst lifetime. Based on the derived scaling relations, we predict the angular sizes and average surface brightnesses of faint galaxies that will be discovered with *JWST*. We find that *JWST* will be able to resolve galaxies at the magnitude limit $m_{\rm AB} < 31$ out to a redshift of $z \sim 14$. The next generation of large ground-based telescopes will resolve all galaxies discovered with *JWST*, provided they are sufficiently clumpy to enable detection above the bright thermal sky. We combine our constraints with simple models for self-regulation of star formation, and show that feedback from supernovae at redshifts $z \gtrsim 3$ is likely mediated through momentum transfer, with the starburst time-scale set by the lifetime of the massive stars rather than the dynamical time in the host galactic disc.

Key words: galaxies: evolution – galaxies: formation – galaxies: high-redshift – cosmology: theory.

1 INTRODUCTION

The luminosity function of Lyman-break galaxy candidates discovered at $z \gtrsim 6$ in the *Hubble* Ultra-Deep Field (HUDF) is described by a Schechter function

$$\Psi(L){\rm d}L = \Psi_\star \left(\frac{L}{L_\star}\right)^\alpha \exp\left(-\frac{L}{L_\star}\right)\frac{{\rm d}L}{L_\star}, \quad (1)$$

where $\Psi_\star$ is the characteristic density in Mpc^{-3} and α is the power-law slope at luminosities L below the characteristic break at $L_\star$. The value of $L_\star$ decreases towards higher redshift as expected from the dark-matter halo mass function (e.g. Muñoz & Loeb 2011), while the faint-end slope of $\alpha \approx -1.8$ is observed to be roughly independent of redshift (McLure et al. 2009; Bouwens et al. 2010; Yan et al. 2010). The luminosity function is the primary observable that must be reproduced by any successful model of galaxy formation (e.g. Salvaterra, Ferrara & Dayal 2010; Trenti et al. 2010; Raičević, Theuns & Lacey 2011).

In a recent study, Oesch et al. (2010) have measured the redshift evolution of the scale-length of galactic discs (see also Ferguson et al. 2004; Bouwens et al. 2004). Among a sample of galaxies with constant luminosity, the half-light galaxy radius was found to scale as

$$R_{\rm gal} \propto (1+z)^{-m}, \quad (2)$$

with $m = 1.12 \pm 0.17$. This evolution is consistent with the inverse relation between virial radius and redshift [$R_{\rm gal} \propto (1+z)^{-1}$] that is expected for dark-matter haloes assuming a constant halo mass-to-luminosity ratio (Ferguson et al. 2004; Oesch et al. 2010).

In this Letter, we model the evolution of galactic disc radii for different parametrized models of self-regulated star formation. We parametrize our models in such a way that the constraints based on the observed size of galaxies are orthogonal to those derived from the slope of the galaxy luminosity function. Based on an empirical determination of parameters of this model, we predict the expected size distribution of galaxies in future surveys with *JWST*, and show that existing observations already set constraints on the physical processes that govern the global properties of star formation at high redshifts. Where required, we adopt the standard set of cosmological parameters (Komatsu et al. 2009), with density parameters $\Omega_{\rm b} = 0.044$, $\Omega_{\rm m} = 0.24$ and $\Omega_\Lambda = 0.76$ for the matter, baryon and dark energy fractional density, respectively, and $h = 0.72$, for the dimensionless Hubble constant.

2 MODEL

To model high-redshift galaxy properties we begin with an expression for the UV luminosity of a galaxy within a dark-matter halo of mass $M_{\rm halo}$,

$$L \propto f_\star M_{\rm halo}\frac{\Omega_{\rm b}}{\Omega_{\rm m}}\frac{\min(t_{\rm SB}, t_\star)}{t_{\rm SB}\, t_\star}, \quad (3)$$

where $f_\star$ is the fraction of baryons turned into stars, $t_{\rm SB}$ is the lifetime of the starburst and $t_\star$ is the average lifetime of the massive stars ($\gtrsim 8\,{\rm M}_\odot$) that affect the feedback through supernova (SN) explosions and dominate the UV luminosity output L. The lifetime

⋆E-mail: swyithe@unimelb.edu.au (JSBW); aloeb@cfa.harvard.edu (AL)

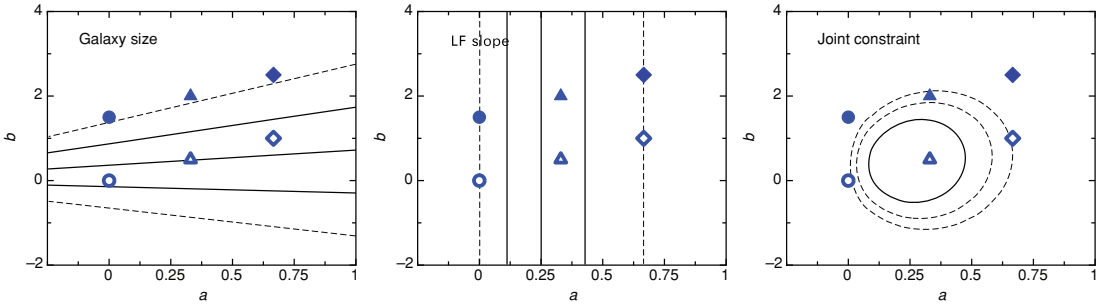

Figure 1. Left-hand panel: contours of parameter combinations (a, b) that give the best-fitting observed value $m = 1.12$ (central solid line), as well as the $\pm1\sigma$ (outer solid lines) and $\pm2\sigma$ combinations (dashed lines). Central panel: contours of parameter combinations (a, b) that give the best-fitting observed value $\alpha' = 0.8$ (central solid line), as well as the $\pm1\sigma$ (outer solid lines) and $\pm2\sigma$ (dashed lines) combinations. Right-hand panel: the combined constraint from the observables m and α, derived from the product of likelihoods $\mathcal{L}_m = \exp[-(m - 1.12)^2/2(0.17)^2]$ and $\mathcal{L}_\alpha = \exp[-(\alpha' - 0.8)^2/2(0.08)^2]$. The contours represent the 32 per cent, 11 per cent and 4.5 per cent likelihoods, which for a Gaussian distribution contain 68 per cent, 90 per cent and 95.4 per cent of the probability, corresponding to the 1σ, 1.5σ and 2σ ranges for parameter pairs. For comparison, the solid and open circles show the example where there is no feedback, but the starburst time-scale is proportional to the dynamical time of the galaxy ($a = 0$, $b = 3/2$) or the average lifetime of massive stars ($a = 0$, $b = 0$), respectively. Similarly, the solid and open diamond points show the example of the model in Wyithe & Loeb (2003) that proposes star formation is limited by the production of the binding energy of the galactic gas in the form of SN-driven winds with $t_{\rm SB} > t_\star(a = 2/3, b = 5/2)$ and $t_{\rm SB} < t_\star(a = 2/3, b = 1)$. Finally, the solid and open triangle points show the example of a model where star formation is limited by SN-driven winds which deposit momentum rather than energy into the galactic gas, with $t_{\rm SB} > t_\star(a = 1/3, b = 2)$ and $t_{\rm SB} < t_\star(a = 1/3, b = 1/2)$.

of main-sequence stars,[1] $t_{\rm ms} = 10^{10}\,{\rm yr}\,(M_{\rm star}/{\rm M}_\odot)^{-2.5}$ (Hansen, Kawaler & Steven 1994), implies an average delay time for SN feedback of $t_\star \sim 7 \times 10^6$ yr for an initial mass function of massive stars ${\rm d}N/{\rm d}M_{\rm star} \propto M_{\rm star}^{-2.35}$ (Scalo 1986). The value of $t_{\rm SB}$ is thought to be related to the dynamical time ($t_{\rm dyn}$) of the galactic disc (Kennicutt 1998), which scales as the age of the Universe $t_{\rm H}$, namely $t_{\rm dyn} \sim 3 \times 10^{-3} t_{\rm H} \approx 3 \times 10^6\,{\rm yr}[(1+z)/7]^{-3/2}$. Here, the constant of proportionality is set by the adiabatic model of Mo, Mao & White (1998). Equation (3) implies that the luminosity could become independent of the starburst lifetime at sufficiently high redshifts $z \gtrsim 3$ for which $t_{\rm dyn} < t_\star$. The mass-to-light ratio is governed by $f_\star$ and $t_{\rm SB}$, each of which can depend on both $M_{\rm halo}$ and z. We therefore parametrize a general class of models for high-redshift galaxy formation using the ratio

$$f_\star \frac{\min(t_{\rm SB}, t_\star)}{t_{\rm SB}\, t_\star} \propto M_{\rm halo}^a (1+z)^b. \quad (4)$$

Physically, this quantity is proportional to the inverse of the mass-to-light ratio. This parametrization can be used to describe a range of physical models that predict the unknown variation of the star formation efficiency and starburst lifetime with redshift and halo mass. Each particular model of the self-regulation of high-redshift star formation will yield distinct values for the parameters a and b.

In order to compare the resulting grid of models with the observed evolution in galaxy size we require two further ingredients, namely the virial relation (simplified form valid at high redshift),

$$M_{\rm halo} \propto R_{\rm vir}^3 (1+z)^3, \quad (5)$$

and the parametrization $R_{\rm gal} \propto R_{\rm vir}$ to describe the relation between virial radius $R_{\rm vir}$ and the galactic disc scale radius $R_{\rm gal}$. In the latter expression, we assume that the disc size is set by the adiabatic model of Mo et al. (1998). We note that flux is detected beyond the galaxy half-light radius in the HUDF observations, and so the galaxy size is not sensitive to the surface brightness threshold. The above set of relations can be used to find the predicted evolution of the galaxy radius with redshift at a fixed luminosity, yielding

$$m = 1 + \frac{1}{3}\frac{b}{a+1}, \quad (6)$$

which can be compared with the observed value of $m = 1.12 \pm 0.17$ (Oesch et al. 2010).

It is also possible to use the observed slope of the luminosity function to constrain the model, thus breaking the degeneracy between the parameters a and b that arises from application of equation (6). Modelling the galaxy luminosity function using the halo mass function (${\rm d}n/{\rm d}M_{\rm halo}$) and the simple parametrized model described in equations (3)–(4), we find

$$\alpha = \frac{{\rm d}\log n}{{\rm d}\log L} = \frac{{\rm d}\log n}{{\rm d}\log M_{\rm halo}} \left|\frac{{\rm d}\log M_{\rm halo}}{{\rm d}\log L}\right| = \frac{1}{a+1}\frac{{\rm d}\log n}{{\rm d}\log M_{\rm halo}}.$$

The host halo masses of faint galaxies observed at $z \gtrsim 6$ is estimated to be $M \sim 10^{10.5}\,{\rm M}_\odot$ (Trenti et al. 2010), for which the mass function has the local power-law slope ${\rm d}\log n/{\rm d}\log M_{\rm halo} \sim -2.5$. At low luminosities the high-redshift ($z \sim 7$) galaxy luminosity function is fitted as a power law with faint-end slope $\alpha = -2$ (McLure et al. 2009; Bouwens et al. 2010). The uncertainty on α is $\sim$10 per cent at $z \gtrsim 7$. We estimate an uncertainty in the value of (${\rm d}\log n/{\rm d}\log M_{\rm halo}$) that is approximately 10 per cent, based on the uncertain mass of the host haloes. We therefore define $\alpha' \equiv \alpha \times ({\rm d}\log n/{\rm d}\log M_{\rm halo})^{-1}$, and adopt the constraint $\alpha' = 1/(a+1) = 0.8 \pm 0.1$ based on equation (7).

2.1 Parameter constraints

The left-hand panel of Fig. 1 shows contours of parameter combinations (a, b) that give the best-fitting observed value $m = 1.12$, as well as the ±1 σ and ±2 σ combinations (equation 6). The central panel of Fig. 1 shows contours of parameter combinations (a, b) that give the best-fitting observed value $\alpha' = 0.8$, as well as the $\pm1\sigma$ and $\pm2\sigma$ combinations. The right-hand panel shows the combined constraint from both observables, with the contours representing the 32 per cent, 11 per cent and 4.5 per cent likelihoods, which for a Gaussian distribution correspond to the 1σ, 1.5σ and 2σ

[1] This approximation becomes inaccurate for very massive stars (Marigo et al. 2008). However the mass-weighted lifetime used here is dominated by the less massive members of the massive star population.

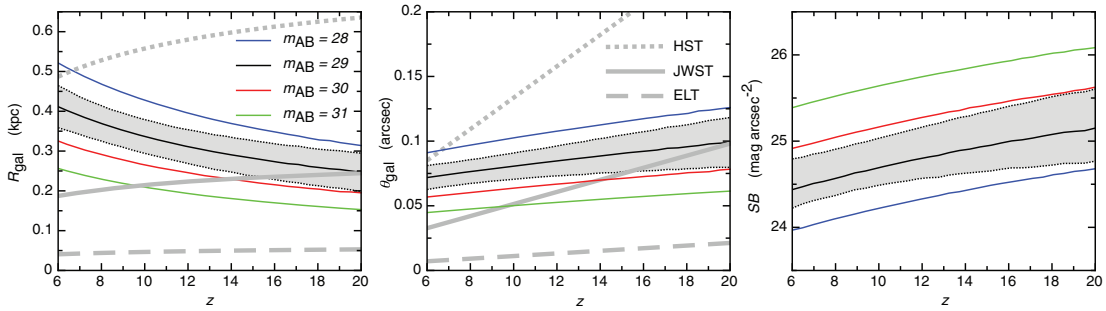

Figure 2. The projected relation between galaxy size and redshift, plotted for four values of apparent magnitude. The left and central panels show the physical (R_{gal}) and apparent angular sizes (θ_{gal}), respectively. For comparison (thick grey lines), we also plot the indicative angular resolution $\Delta\theta$ of telescopes with diameters corresponding to *HST* ($D_{tel} = 2.5$ m), *JWST* ($D_{tel} = 6.5$ m) and ELT ($D_{tel} = 30$ m). The right-hand panel shows the relation between surface brightness (averaged within the scale radius) as a function of redshift. In each panel, the grey band around the case of $m_{AB} = 29$ mag shows the 68 per cent range of uncertainty on the mean.

regions for parameter combinations. We find $a = 0.3 \pm 0.15$ and $b = 0.5 \pm 0.6$ (68 per cent range on individual parameters).

3 THE SIZE OF HIGH-REDSHIFT GALAXIES

Our empirical constraints can be used to extrapolate galaxy size out to the higher redshifts and lower luminosities that will be observed by the next generation of telescopes. Beginning with equations (3)–(4) we get $L \propto M_{halo}^{a+1}\,(1+z)^b$, which when combined with equation (5) and the parametrization $R_{gal} \propto R_{vir}$ implies

$$R_{gal} \propto L^{\frac{1}{3(1+a)}}(1+z)^{-(1+\frac{b}{3(1+a)})} \propto L^{\frac{1}{3(1+a)}}(1+z)^{-m}$$
$$= R_0 \left(\frac{D_L(z)}{D_L(z_0)}\right)^{\frac{2}{3(1+a)}} 10^{\frac{m_{AB,0}-m_{AB}}{7.5(a+1)}} \left(\frac{1+z}{1+z_0}\right)^{-m}, \quad (7)$$

where D_L is the luminosity distance, m_{AB} is the apparent galaxy magnitude and $m_{AB,0}$ is the apparent magnitude of galaxies from which the normalization of the relation (R_0) is measured at redshift z_0. The normalization of this relation is calibrated using observed galaxy sizes at $z \sim 7$–8 (Oesch et al. 2010). We average the prediction over the three independent points[2] having (z_0, R_0, $m_{AB,0}$) = (7, 0.5 ± 0.1, 27.8), (7, 0.75 ± 0.1, 26.6) and (8, 0.4 ± 0.1, 28.1), and over distributions $m = 1.12 \pm 0.17$ and $\alpha = 0.3 \pm 0.15$. The resulting relation is shown in Fig. 2 as a function of redshift for four values of apparent magnitude. In the case of $m_{AB} = 29$ mag, the grey band shows the 68 per cent range of uncertainty on the mean radius. The left and central panels show the physical and apparent angular sizes (θ_{gal}), respectively. Galaxies of fixed apparent magnitude have smaller physical sizes (but larger angular sizes) at higher redshift.

For comparison, we also plot in Fig. 2 the indicative angular resolutions of telescopes with diameters corresponding to *HST* ($D_{tel} = 2.5$ m), *JWST* ($D_{tel} = 6.5$ m) and an extremely large telescope (ELT; $D_{tel} = 30$ m)

$$\Delta\theta = \frac{1.22\lambda}{D_{tel}} \approx 0.085 \left(\frac{1+z}{7}\right)\left(\frac{D_{tel}}{2.5}\right)^{-1}. \quad (8)$$

Here, we have calculated the resolution at the observed wavelength of the redshifted Lyα line $\lambda = 1216\,(1+z)$ Å. This simple comparison suggests that galaxies with an apparent magnitude of $m_{AB} = 28$ mag (1 mag brighter than the *HST* WFC3/IR limit) have an angular size of $\theta_{gal} \sim 0.1$ arcsec, which is at the limit of *HST* resolution (Oesch et al. 2010). Fainter galaxies at higher redshifts cannot be resolved by *HST*. The larger aperture of *JWST* will allow the study of galaxy structure at higher redshift and fainter fluxes (Windhorst et al. 2008). For example, galaxies with $m_{AB} = 29$ mag will be resolved out to at least $z \gtrsim 15$. Moreover, *JWST* will be able to resolve galaxies at the magnitude limits of $m_{AB} < 30$ and $m_{AB} < 31$ out to $z \sim 10$ and $z \sim 14$, respectively. Galaxies at yet higher redshifts or fainter fluxes would appear point-like. Bright galaxies are known to become rarer towards high redshift (e.g. Bouwens et al. 2010; Yan et al. 2010), and the discovery of such very high redshift galaxies by *JWST* could be limited by its relatively small field of view (e.g. Muñoz & Loeb 2011). However, our extrapolation suggests that an ELT would be able to resolve all galaxies detectable with *JWST*.

The above discussion refers only to angular resolution and neglects surface brightness sensitivity. Calculation of the details of surface brightness sensitivity (see e.g. Windhorst et al. 2008) is beyond the scope of this Letter. However, we note that faint, high-redshift galaxies are always below the surface brightness of the sky. Therefore, in order to measure the details of a high-redshift galaxy profile, an *HST* observation must achieve a very high signal-to-noise ratio on the zodiacal sky (of the order of 10^3 per pixel) so that the background would be reliably subtracted (Hathi et al. 2008). The right-hand panel of Fig. 2 shows the average surface brightness within the scale-radius of galaxies of various magnitudes as a function of redshift. Galaxies with $m_{AB} = 29$ mag show ∼24.5 mag per arcsec^2 at $z \sim 6$, becoming fainter by only a modest amount towards $z \sim 20$. The plotted curves should be compared to the space-based value for the zodiacal sky in the *K* band of ∼22.5 mag per square arcsec^2 (Windhorst et al. 2010), or the ground-based *K*-band value of ∼14 mag per arcsec^2 for the thermal sky. The difference in sky brightness between the ground and space implies that *HST* is equivalent in sensitivity (but not in resolution) to a 150-m ground-based telescope for the purpose of imaging resolved high-redshift galaxies. Thus, a ground-based ELT will not be competitive with *HST* or *JWST*, since it must overcome the much brighter sky. As a result, even though all high-redshift galaxies discovered with *JWST* could be resolved by an ELT, their surface brightness will render their extended structure undetectable. However, high-redshift galaxies are observed to be very clumpy owing to the presence of star-forming regions (Hathi et al. 2008), and an ELT will be more sensitive to these unresolved clumps than to diffuse structure, owing to the higher resolution in addition to larger collecting area. Indeed, *HST* is comparable to *only* a 20-m ground-based telescope with respect

[2] Uncertainty in R_0 is the standard error on the mean.

to point source sensitivity (but without the resolution of a 20 m aperture). Thus, if high-redshift galaxies are sufficiently clumpy, then an ELT may be able to obtain close to the theoretical resolution shown in the central panel of Fig. 2.

4 STAR FORMATION MODEL CONSTRAINTS

A range of simple models for the process governing star formation can be compared to the constraints on parameters a and b. We consider three simple models for the possible feedback. The first is a model where there is no self-regulation of star formation. The second and third models describe the evolution in cases where the star formation is limited by SN feedback, and the interaction between the SN-driven wind and the galactic gas conserves energy and momentum, respectively. In each of these three cases, we consider scenarios where the lifetime of the starburst is proportional to the galaxy dynamical time and to the lifetime of massive stars, respectively. Altogether, we have six model predictions for m and α' with which to compare our constraints.

4.1 Models without feedback

We begin with feedback-free models in which the star formation efficiency $f_\star \propto M_\star/M_{\rm halo} = {\rm const}$. We first consider the case where the natural time-scale for the starburst is proportional to the galaxy dynamical time, $t_{\rm SB} \propto t_{\rm dyn} \propto (1+z)^{-3/2}$, which implies

$$f_\star \frac{\min(t_{\rm SB}, t_\star)}{t_{\rm SB}\, t_\star} \propto \frac{f_\star}{t_{\rm dyn}} \propto \frac{M_{\rm halo}^0 (1+z)^0}{(1+z)^{-3/2}} \propto M_{\rm halo}^0 (1+z)^{3/2}, \quad (9)$$

yielding $a = 0$ and $b = 3/2$. This parameter combination is shown by the solid circles in Fig. 1 for comparison with the present constraints. We find that this simple model is inconsistent with both the observed evolution in $R_{\rm gal}$ and the observed luminosity function slope at the 2σ level. The combined constraint rules out this model at high confidence.

However, at high redshifts when the dynamical time is shorter than the average lifetime of massive stars, the same luminosity may be achieved with a lower star formation rate than in the model described above,

$$f_\star \frac{\min(t_{\rm SB}, t_\star)}{t_{\rm SB}\, t_\star} \propto \frac{f_\star}{t_\star} \propto M_{\rm halo}^0 (1+z)^0, \quad (10)$$

yielding $a = b = 0$ for galaxies in this case. Such a model (shown by the open circular symbols) is ruled out by the slope of the luminosity function at the 2σ level, but is consistent with the observed evolution in galaxy radius. The combined constraint rules out this model at high confidence.

4.2 Models with feedback through energy conservation

We next consider models including self-regulation of star formation by SN feedback. The model of Wyithe & Loeb (2003) assumes that star formation is limited by the transfer of energy from SN-driven winds when it is equal to the binding energy to the galactic gas (Dekel & Woo 2003). The model asserts that stars form with an efficiency $f_\star$ out of the gas that collapses and cools within a dark-matter halo and that a fraction $F_{\rm SN}$ of each SN energy output, $E_{\rm SN}$, heats the galactic gas mechanically. The mechanical feedback will halt the star formation once the cumulative energy returned to the gas by SNe equals its binding energy (assuming negligible radiative losses for a sufficiently rapid starburst). Hence, in this model the limiting stellar mass is set by the condition

$$\frac{M_\star}{w_{\rm SN}} E_{\rm SN} F_{\rm SN} = E_{\rm b} = \frac{1}{2}\frac{\Omega_{\rm b}}{\Omega_{\rm m}} M_{\rm halo} v_{\rm c}^2, \quad (11)$$

where $E_{\rm b}$ is the binding energy of baryons in the galaxy, $w_{\rm SN}$ is the mass in stars (in $\rm M_\odot$) per SN explosion and $v_{\rm c}$ is the halo circular velocity. Equations (5) and (11) imply that the total mass in stars, $M_\star = (f_\star \Omega_{\rm b}/\Omega_{\rm m}) M_{\rm halo}$, scales as

$$M_\star \propto M_{\rm halo}^{5/3} (1+z), \quad (12)$$

and hence the star formation efficiency scales as $f_\star \propto M_{\rm halo}^{2/3}\,(1+z)$. Thus, smaller galaxies are less efficient at forming stars, but a galaxy of fixed mass is more efficient at forming stars at higher redshift.

In a model where the starburst lifetime is proportional to the galaxy dynamical time, we find

$$\frac{f_\star}{t_{\rm dyn}} \propto \frac{M_{\rm halo}^{2/3}(1+z)}{(1+z)^{-3/2}} \propto M_{\rm halo}^{2/3} (1+z)^{5/2}. \quad (13)$$

This model can therefore be parametrized in terms of the combination $a = 2/3$, and $b = 5/2$ for galaxies, which is shown by the solid diamonds in Fig. 1. This simple SN-driven feedback model is inconsistent with the observed evolution in $R_{\rm gal}$ and the luminosity function slope at the $2\,\sigma$ level. The combined constraint rules out this model at high confidence.

However, at high redshifts $z \gtrsim 3$ when the disc dynamical time is shorter than the lifetime of a massive star $t_\star \sim 10^7$ yr, we note that SN feedback will be less efficient, and the star formation efficiency could exceed the self-regulated value of $f_\star$ described above. In particular,

$$\frac{f_\star}{t_\star} \propto \frac{M_{\rm halo}^{2/3}(1+z)}{t_\star} \propto M_{\rm halo}^{2/3} (1+z), \quad (14)$$

yielding $a = 2/3$, and $b = 1$ for galaxies in this case (open diamond symbols). Such a model is consistent with the observed evolution of galaxy size, but inconsistent with the slope of the luminosity function at the 2σ level.

4.3 Models with feedback through momentum conservation

Finally, we consider a model where the SN-driven winds conserve momentum in their interaction with the galactic gas rather than energy. In this case the limiting stellar mass is set by the condition

$$\frac{M_\star}{w_{\rm SN}} \frac{E_{\rm SN}}{c} F_{\rm SN} = \frac{1}{2}\frac{\Omega_{\rm b}}{\Omega_{\rm m}} M_{\rm halo} v_{\rm c}. \quad (15)$$

In a model where the starburst time-scale is proportional to the galaxy dynamical time, we find

$$\frac{f_\star}{t_{\rm dyn}} \propto M_{\rm halo}^{1/3} (1+z)^2. \quad (16)$$

This model (solid triangles), represented by $a = 1/3$ and $b = 2$, is consistent with the constraints from α, but ruled out at the 2σ level by the constraints from the evolution of galaxy radius. If instead the lifetime of massive stars sets the starburst time-scale, we find

$$\frac{f_\star}{t_\star} \propto M_{\rm halo}^{1/3} (1+z)^{1/2}, \quad (17)$$

which is represented by $a = 1/3$ and $b = 1/2$, and is plotted as the open triangles in Fig. 1. This model is consistent with both the constraints from m and α'.

Our results imply that SN feedback in high-redshift galaxies occurs through the transfer of momentum between the SN-driven wind and the galactic gas, and that the starburst time-scale is set by the average lifetime of massive stars rather than the dynamical time of the host galactic disc. However before concluding we note the caveat that our modelling implicitly assumes an IMF that is not evolving with redshift, whereas a redshift dependent IMF could imply evolution of both the mass-to-light ratio and the fraction of stellar mass per SN explosion. Inclusion of this possibility may modify the conclusions reached here.

5 DISCUSSION

We have used the observed redshift evolution of disc sizes, and luminosity function of galaxies, to constrain the relationship between star formation efficiency and starburst lifetime. Assuming a constant IMF, we find that SN feedback in high-redshift galaxies is likely mediated through momentum transfer with the starburst time-scale dictated by the average lifetime of massive stars, $t_\star$. The latter result follows naturally from the fact that the dynamical time of galactic discs becomes shorter than $t_\star \sim 10^7$ yr at redshifts $z \gtrsim 6$.

We extrapolated the derived scaling relations to predict the angular sizes of galaxies at higher redshifts and fainter fluxes than currently observed. We have found that *JWST* will be able to resolve galaxies with $m_{\rm AB} < 30$ and $m_{\rm AB} < 31$ only out to redshifts of $z \sim 10$ and $z \sim 14$, respectively. However, if high-redshift galaxies are sufficiently clumpy, so that unresolved star-forming regions can be detected above the bright thermal sky, then the next generation of ground-based ELTs will be able to resolve structure in all galaxies at all redshifts detectable by *JWST*.

ACKNOWLEDGMENTS

We thank Rogier Windhorst for helpful comments and discussion. JSBW acknowledges the support of the Australian Research Council. AL was supported in part by NSF grant AST-0907890 and NASA grants NNX08AL43G and NNA09DB30A.

REFERENCES

Bouwens R. J. et al., 2004, ApJ, 611, L1
Bouwens R. J. et al., 2010, preprint (arXiv:1006.4360)
Dekel A., Woo J., 2003, MNRAS, 344, 1131
Ferguson H. C. et al., 2004, ApJ, 600, L107
Hansen C. J., Kawaler S. D., 1994, Stellar Interiors: Physical Principles, Structure, and Evolution. Springer-Verlag, Berlin, p. 28
Hathi N. P. et al., 2008, AJ, 135, 156
Kennicutt R. C., Jr, 1998, ApJ, 498, 541
Komatsu E. et al., 2009, ApJS, 180, 330
Marigo P. et al., 2008, A&A, 482, 883
McLure R. J. et al., 2009, MNRAS, 395, 2196
Mo H. J., Mao S., White S. D. M., 1998, MNRAS, 295, 319
Muñoz J. A., Loeb A., 2011, ApJ, 729, 99
Oesch P. A. et al., 2010, ApJ, 709, L21
Raičević M., Theuns T., Lacey C., 2011, MNRAS, 410, 775
Salvaterra R., Ferrara A., Dayal P., 2010, preprint (arXiv:1003.3873)
Scalo J. M., 1986, Fund. Cosmic Phys., 11, 1
Trenti M. et al., 2010, ApJ, 714, L202
Windhorst R. A. et al., 2008, Adv. Space Res., 41, 1965
Windhorst R. A. et al., 2010, preprint (arXiv:1005.2776)
Wyithe J. S. B., Loeb A., 2003, ApJ, 595, 614
Yan H.-J. et al., 2010, Res. Astron. Astrophys., 10, 867

This paper has been typeset from a TEX/LATEX file prepared by the author.